Journal of Alloys and Compounds 476 (2009) 683–688

Contents lists available at ScienceDirect

Journal of Alloys and Compounds

journal homepage: www.elsevier.com/locate/jallcom

Microstructure and phase transition of biocompatible titanium oxide film on titanium by plasma discharging

Chiung-Fang Huang[a,b], Hsin-Chung Cheng[a,b], Chung-Ming Liu[c,d], Chang-Chih Chen[a,e], Keng-Liang Ou[a,f,g,*]

[a] School of Dentistry, College of Oral Medicine, Taipei Medical University, Taipei 110, Taiwan
[b] Department of Dentistry, Taipei Medical University Hospital, Taipei 110, Taiwan
[c] Department of Chemical and Material Engineering, LungHwa University of Science and Technology, Taoyuan, Taiwan
[d] Graduate School of Engineering, LungHwa University of Science and Technology, Taoyuan, Taiwan
[e] Department of Emergency Medicine, Mackay Memorial Hospital, Taipei 110, Taiwan
[f] Graduate Institute of Biomedical Materials and Engineering, College of Oral Medicine, Taipei Medical University, Taipei 110, Taiwan
[g] Research Center for Biomedical Implants and Microsurgery Devices, Taipei Medical University, Taipei 110, Taiwan

ARTICLE INFO

Article history:
Received 14 July 2008
Received in revised form 3 September 2008
Accepted 14 September 2008
Available online 21 January 2009

Keywords:
Titanium
Oxidation
Plasma discharging

ABSTRACT

This study investigated the feasibility of using oxygen plasma discharging on titanium for forming a biocompatible layer between the bone plate and bone tissue. Plasma discharging formed a nanostructural oxidation layer on the titanium bone plate. The nanostructural oxidation layer revealed oxygen and titanium bonding states following oxygen plasma discharging. A ($\alpha \rightarrow (\alpha + TiO) \rightarrow (\alpha + TiO + \gamma\text{-}TiO_2)$) phase transition was observed within the titanium matrix during plasma discharging. This result has never been previously reported. The plasma oxidation with argon pretreatment not only produces titanium oxide layer, but also results in formation of nanostructural titanium oxide phase. Nano-rutile-TiO_2 (γ-TiO_2) can be enhanced osseointegration of implant such as orthopedic and dental implants. In addition, nano-($TiO + \gamma$-TiO_2) phases were formed on the nanostructural oxidation layer by plasma discharging. Formation of a nanostructural rutile-TiO_2 on oxidation layer is related with the cell and blood reaction and distribution selectivity, then promoting hemocompatibility and protein binding as well as osseointergration. Therefore, surface oxidation by plasma discharging is thus believed to improve the biocompatibility and tissue healing. Furthermore, plasma discharging not only enhances phase transformation on titanium surface, but also generates a nanostructural oxide layer, improving the bioactivity and hemocompatibility of bone plate.

1. Introduction

Titanium-based implants are widely applied in orthopedics and dentistry owing to their superior biocompatibility and mechanical properties. The biological property of titanium is attributed to its surface oxide film. The passive oxide film formed naturally in atmosphere is dense and stable anatase titanium oxide film with a thickness of approach a few nanometers, which results in excellent anti-corrosion capability of titanium. However, titanium-based alloys are usually bioinert and poor integration with tissue, even though a direct bone-implant contact called osteointegration could be formed [1,2]. Several researches have been considerable efforts for improving the bioactivity of titanium [3–7]. Furthermore, in an effort to enhance the cell-implant material interaction and increase lifetime, bioactive ceramic-based coatings have been applied to titanium-based implants. Among of them, hydroxyapatite (HA) has been suggested as a potential material to implant coating [8–10]. However, it is well known that one problem with HA coatings is poor adhesion strength at the HA/implant interface [11]. Recently, titanium oxide has been applied as a potential alternative to HA coatings. The advantage of titanium oxide (TiO_2) is that it can be formed directly on implant surface, by wet process such as anodization and acid immersion [3–7,12,13]. TiO_2 is formed with a chemical bond between the oxide and Ti implant that results in improving adhesion strength. Even though TiO_2 film can be grown directly on Ti surface by cost-effective techniques, the implant cleaning after chemical treatments and resulting in environment pollution are problems to be solved urgently. Plasma modification is commonly

* Corresponding author at: Graduate Institute of Biomedical Materials and Engineering, College of Oral Medicine, Taipei Medical University, Taipei 110, Taiwan.
Tel.: +886 2 27361661x5400; fax: +886 2 27362295.
E-mail address: klou@tmu.edu.tw (K.-L. Ou).

0925-8388/$ – see front matter © 2008 Elsevier B.V. All rights reserved.
doi:10.1016/j.jallcom.2008.09.122

applied to functionize the biomaterials and materials [14–19]. The feasibility of using glow discharge plasma treatments for sterilizing implants has also been demonstrated [13]. Therefore, surface modification is essential to upgrade the performance of biomaterials by depositing plasma-polymerized thin films. The plasma process provides a simple, completely dry, *in situ* process for chemically tailoring surfaces without compromising the inherent, favorable bulk properties of the biomaterials. Although plasma procedures have been extensively adopted in biomaterials research [14,15], studies on mechanisms for surface cleaning and modifying biomaterials are rare. Therefore, in addition to investigating the possibilities and limitations of plasma techniques for controlled cleaning and modification of titanium surfaces. This study examines the feasibility of using surface modification to enhance the performance of biomaterials via plasma discharging. The properties of treated and untreated titanium plates are evaluated by material analysis and biocompatibility tests.

2. Experimental procedures

2.1. Preparation of Ti, O–Ti-1 and O–Ti-2

The Grade IV titanium substrates used in these experiments were 2-mm thick 1-cm diameter plates with 99.7% purity (Hung Chung Bio-S Co. Ltd., Kaoshiung Science Park, Taiwan). The titanium plates were polished using SiC metallographic papers. After polishing, specimens were cleaned with methylethylketone for 5 min, washed in distilled water for 20 min, acid pacified in 30% nitric acid for 30 min according to the American Standard Testing Materials (ASTM) procedure and rinsed again in ultrapure water for 20 min. The samples were subjected to argon-plasma treatment in the vacuum reactor. Plasma cleaning was performed at a discharge power of 200 W, a working pressure of 250 mTorr, and an argon flow rate of 20 sccm, after reducing the base pressure to below 500 mTorr. The plates were then subjected to oxygen plasma treatments following 500 W from 5 min to 30 min. *In situ* plasma oxidation was performed again when the base pressure decreased below 500 mTorr. For easy identification, pure Ti, Ti with 15 min-oxygen plasma treatments and Ti with 30 min-oxygen plasma treatments were denoted as Ti, O–Ti-1 and O–Ti-2, respectively.

2.2. Properties evaluation of Ti, O–Ti-1 and O–Ti-2

To estimate the properties of Ti, O–Ti-1 and O–Ti-2, the surface morphologies were analyzed by atomic force microscope (AFM) with a Si probe. Surface compositions and binding states of Ti, O–Ti-1 and O–Ti-2 were analyzed by X-ray photoemission spectroscopy (XPS) with a monochromatic Ag Kα source. The X-ray power was 250 W. Moreover, the XPS energy scale was calibrated by setting the binding energy of the $Ag_{3d5/2}$ line of clean silver to precisely 368.3 eV. High-resolution scans were performed for Ti, and O using an X-ray beam with a diameter of approximately 15-nm. Secondary ion mass spectroscopy (SIMS) was applied to analyze the compositional depth profiles of plasma-treated titanium bone plates. An O_2^+ primary ion beam with impact energy of 3 keV was applied. Resistivity measurements of Ti, O–Ti-1 and O–Ti-2 were taken using a four-point probe system.

2.3. Biocompatibility of Ti, O–Ti-1 and O–Ti-2

To evaluate the biocompatibility of Ti, O–Ti-1 and O–Ti-2, the test specimens (10 mm × 10 mm × 1 mm) were cell cultured (MG-63), and cell morphology and proliferation were observed. The test specimens were placed in a 24-well polystyrene plate. Before cell culture, all specimens were exposed to ultraviolet (UV) radiation for 24 h. The test specimens were sterilized and washed several times with Dulbecco modified Eagle medium (DMEM, Gibco) and phosphate-buffered saline (PBS, 0.1 M, pH 7.2). The culture medium consisted of DMEM containing 10% fetal bovine serum (FBS), 100 mg/ml of streptomycin and 100 U/ml of penicillin. The MG-63 cell suspension with a $3 \times 10^4/cm^2$ density was added into the plate. A 500 ml culture solution and 50 ml 3-[4,5-dimethylthiazol-2-yl]-2,5-diphenyltetrazolim bromide (MTT) label solution were added to each culture well the plate was then placed in a culture chamber at 37 °C in a humidified atmosphere of 95% air and 5% CO_2. The culture medium was changed every 3 days. The test specimens were cultured for the following periods: 8 h, 24 h, 36 h and 48 h. The extent of adhesion and proliferation of MG-63 cells on the treated surfaces of various Ti-alloys were evaluated by observing cell morphologies with SEM, calculating cell count with hemocytometer and performing MTT assay to obtain the cell optical density (OD) by the plate reader (ELISA, DYNEX-MRX II) at λ = 595 nm.

3. Results and discussion

Fig. 1 shows the RMS surface roughness as a function of plasma-treated time. The surface roughness was assessed by AFM. The surface became smoother with longer plasma-treatment. The surface roughness of Ti, O–Ti-1 and O–Ti-2 plates were 420.5 nm, 55.4 nm and 38.2 nm, respectively. The titanium plate without any treatment is existed rough surface owing to the polishing procedure. The surface roughness of titanium plate decreased as increasing plasma treatment time. Sputtering and/or stuffing effects are believed to be caused by the reactions or bombardment of energetic radicals and ions during plasma treatment. The titanium surfaces are sputtered to make them smooth and no impurity particles were observed on the plasma-treated surface. The above observations indicate that plasma treatment reduced the surface contamination. This observation is in agreement with other previous studies [20]. Additionally, more surface areas were provided for cell attachment with increased surface oxidation. Increases in the both surface area available for binding and the microtexture are believed to improve bioactivity and thus improve the rate of bone formation [21–24].

Fig. 2 presents TF-XRD spectra of Ti, O–Ti-1 and O–Ti-2. For the Ti, only strong Ti peaks were detected. The crystalline structure of the O–Ti-1 and O–Ti-2 was composed of Ti and TiO_2 phases. These experimental results were consistent with Cheng et al. [6] and Cheng and co-workers [7]. The anatase TiO_2 was also investigated for Ti following anodization with cathodic pretreatment. Titanium oxide film is known to form naturally in air and stable titanium oxide (anatase TiO_2) is a few nanometers thick [7]. The TF-XRD pattern analyses of O–Ti clearly revealed the reflection peak of anatase structure and crystalline structure, which indicates that ion bombardment, induces phase transformation during plasma oxidation. Osteogenic cells are known to interact not with the titanium implant surface itself, but with a blood-modified titanium oxide surface. Coagulation is the first step of bone healing. Titanium oxide film with 3D micro/nanoporous structure may enhance apatite formability as compared to dense titanium oxide, then increasing adsorption rate of albumin/fibrinogen [25].

The thickness of TiO_2 on Ti and O–Ti-2 was further observed by cross-sectional TEM. Fig. 3(a) shows micrograph of Ti without any treatment. The thin oxide layer (~10 nm) was observed. Furthermore, it revealed that O diffused toward the Ti surface after plasma oxidation. Oxide thickness of O–Ti-2 is above 400 nm (Fig. 3(b)). The O–Ti-2 specimen has the thicker oxide layer than Ti, and O–Ti-1. The biomedical implants and plates with passive oxide film possess high biocompatibility [26,27]. Titanium anodized in H_2SO_4 solution showed enhancement of oxide growth and increase of osseointegration [6–8]. Titanium-based biomedical implants have indicated that the thickness of the oxide layer increases with time on implant surface and the ions (Ca, P, S) from the physiological environment as incorporated into the oxide layer [14]. As stated above, it is believed that plasma oxidation on titanium-based implants and bone plates can enhance biocompatibility and osseo/osteointegration than without plasma oxidation. In addition, even if the amorphous-like oxide film was formed by plasma discharging in the present study, the variations of phase transition are investigated during plasma oxidation by field-assisted migration of ions in glow discharging systems and the oxygen ion and species can be accelerated to overcome the barrier of surface energy, resulting in the phase transformation on oxide film. Namely, Oxygen plasma treatment also enhances the Ti incorporation. A high density of excited and unstable species, like ions and radicals, is produced in the plasma, which constitutes a powerful reactive atmosphere. Moreover, because of their acceleration in the plasma sheath, the ionic species impinging on the surface have

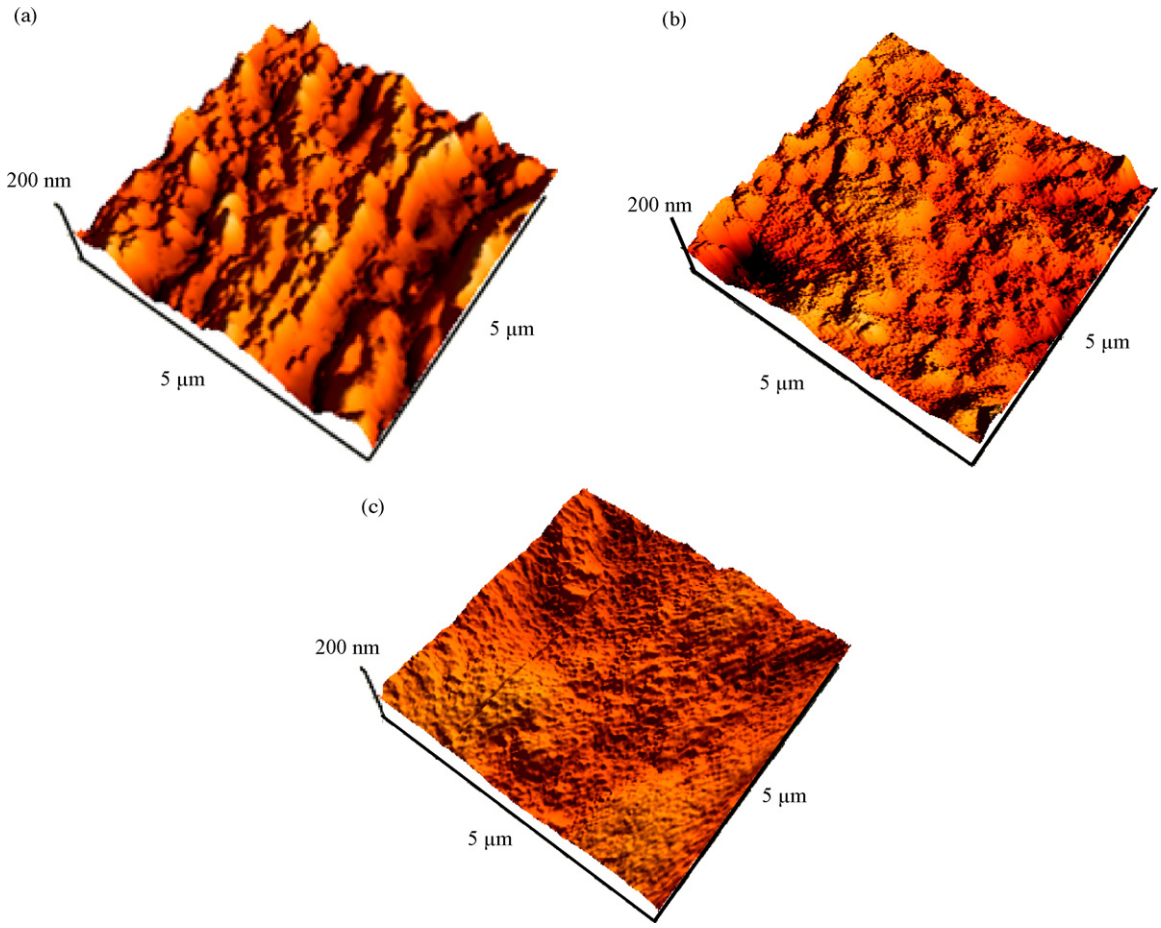

Fig. 1. AFM images of titanium plates, (a) Ti, (b) O–Ti-1 and (c) O–Ti-2.

some kinetic energy, which enhances the activation of surface reactions. Amorphous titanium oxide transformed into polycrystalline and/or crystal structure as the plasma treatment time increased during plasma discharging. It is believed that polycrystalline and/or crystal titanium oxide can be improved the bioactivity on biomedical implant surfaces [28]. Furthermore, the nanostructure and nanophase ceramics such HA, TiO, TiO_2 and Al_2O_3 can enhance long-term osteoblast functions relative to microstructural variations [29].

Fig. 3(b) presents TEM micrographs and selected-area diffraction patterns (SADPs) of O–Ti-2. It shows various microstructures in the amorphous-like oxide layer (~400 nm). Fig. 3(b) also reveals an FFT analysis in the area denoted as area A. Area A has no diffraction spots, indicating that the amorphous-like metal oxide formed on the oxidation layer. Fig. 3(c) displays the image, taken from the high resolution transmission electron microscopy (HRTEM) and performed by FFT analysis, the *d*-spacing of the plane (0 1 1) for TiO was equal to 0.238–0.242 nm. Similar result was also observed in previous study [30]. Fig. 3(b) also shows a SADP taken from area B. B appears in spots instead of in a ring pattern, indicating that B-area is a nanostructure. The FFT analysis and the camera length and *d*-spacings of the reflection spots reveal a diffraction ring pattern of the plate-like precipitate (denoted as B in Fig. 3(b)). The first, second and third rings correspond to the titanium oxide {1 1 1}, {1 0 1} and {2 1 0} planes, respectively. The crystal structure of the plate-like precipitate was determined to be rutile-TiO_2 (γ-TiO_2) with a bct structure and lattice parameter $a = 4.61$ nm and $c = 3.12$ nm. No phases other than the oxygen deficient titania were found in the oxide film. Based on the results of Fig. 3, it indicated that the surface oxide layer was also existed crystalline and amorphous oxide structure. In comparison to the TF-XRD results, the phase transformation of specimens from amorphous to rutile is obvious as plasma treated time increases. The variations of surface microstructure are determined during the plasma discharging by field-assisted migration of ionization systems. This can be explained the outer oxidation layer is mixture structure (amorphous and nanocrystalline TiO and TiO_2), indicating not only that the nanophase formed during glow-discharging reactions, but also that ion/electro-bombardment was responsible for nanocrystallization.

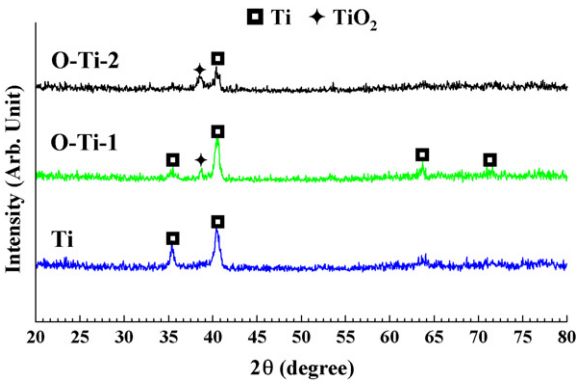

Fig. 2. TF-XRD spectra of Ti, O–Ti-1 and O–Ti-2.

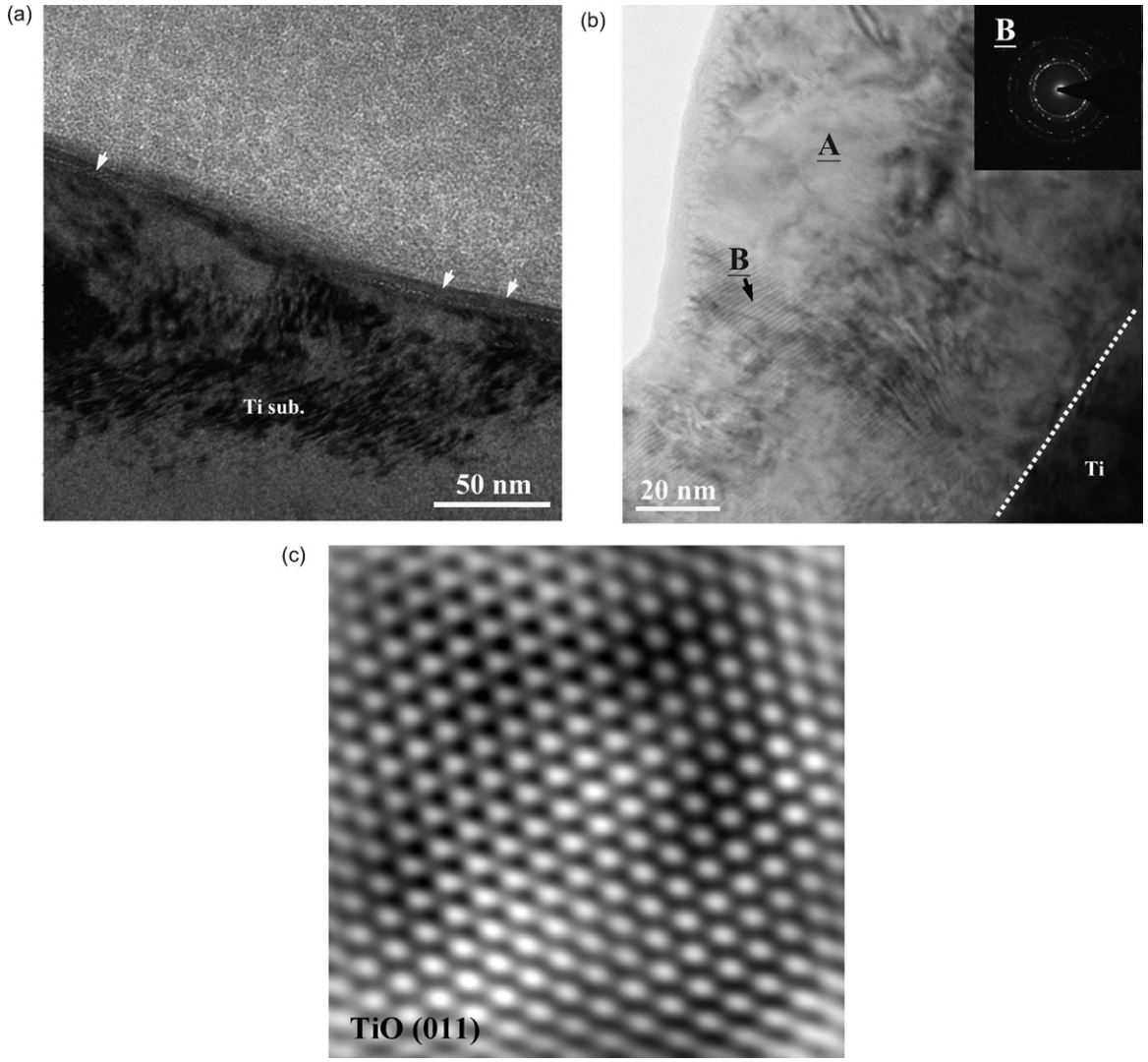

Fig. 3. TEM micrographs and selected-area diffraction patterns (SADPs) of (a) Ti, (b) O–Ti-2 and (c) TiO.

Fig. 4 shows the variations of oxygen concentration on Ti and O–Ti-2. The oxygen concentration in the oxide layer of Ti with and without plasma oxidation was also further examined by SIMS. The concentration of oxygen increased as the Ar ions became sputtered on the oxide film. The O diffused toward the Ti surface after plasma oxidation. The diffused thickness of the oxide film exceeded ~350 nm. The O–Ti-2 had a thicker oxide layer than the Ti. The implant biomaterials with thick oxide layers had better biocompatibility [6–8,19–21]. Oxide films pretreated in H_2O_2 enhance oxide growth and increase adsorption of plasma proteins [7]. For titanium-based implants, the thickness of the surface oxide layer increases with time and increased concentration of ions incorporated into the growing oxide from the physiological environment [13]. Hence, O–Ti implant alloy is believed to have better biocompatibility and osseointegration than Ti without plasma oxidation.

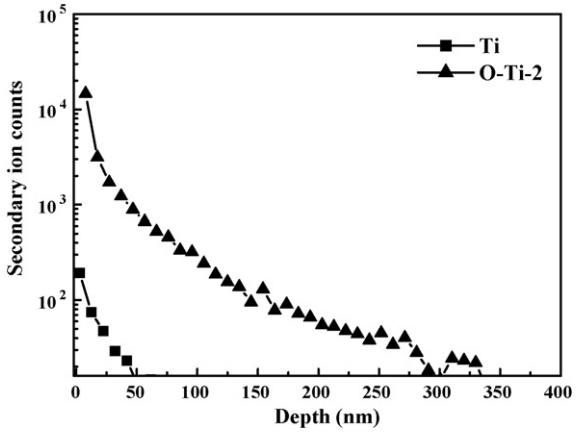

Fig. 4. SIMS depth profile of Ti and O–Ti-2.

The relationship between plasma-treated time and resistivity was also investigated. As the treated time of oxygen plasma increased to 30 mins, the resistivity increased obviously, which was due to oxygen incorporated with titanium. This finding also indicates that the longer the time of the plasma treatment, the lower conductivity the implant surface. The formation of the amorphous layer would increase the resistivity due to increasing scattering effects. The variation in resistivity is due to the oxygen incorporation and formation of amorphous structure. The oxygen incorporation is the dominant factor in the early plasma discharging. Resistivity would increase due to the development of the amorphous layer after increasing plasma discharging. As stated

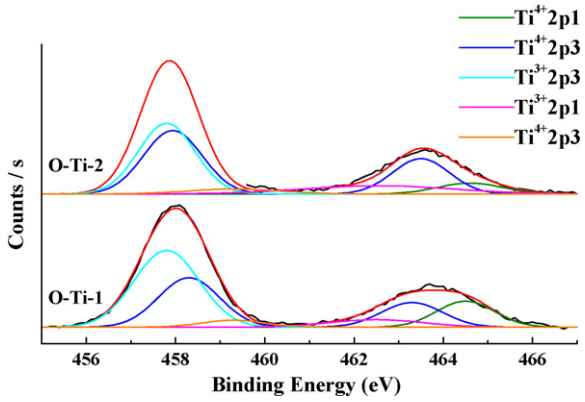

Fig. 5. Ti 2p XPS spectra of O–Ti following various plasma powers.

above, oxygen concentration is related with formation of amorphous layer and resistivity variation. It is believed that the thickness of the oxide layer increased as plasma time increased, and the thick oxide layer has a more hydrophilic capability. Furthermore, plasma oxidation produces a hydrophilic surface, enhancing tissue healing [7,10,28].

Fig. 5 shows the results of curve fitting on the Ti 2p and O 1 s spectra of O–Ti-1 and O–Ti-2. Fig. 5(a) shows a computer-assisted Gaussan–Lorentzian peak model applied to curve fitting of the Ti 2p spectra. The non-plasma-treated titanium oxide films exhibited Ti^{2+}, Ti^{3+} and Ti^{4+} chemical states. As in the O–Ti-1 and O–Ti-2 surface, the valence states of the Ti^{4+} increased, but those of Ti^{2+} and Ti^{3+} decreased. This suggests that the oxide layer component TiO_2 increased, but TiO and Ti_2O_3 decreased. In the O–Ti-1 specimen, the binding energy of $Ti2p_{3/2}$ and $Ti2p_{1/2}$ were located at 457.5 eV and 463 eV, which were assigned to TiO and Ti_2O_3, respectively. For O–Ti-2 specimen, the $Ti2p_{3/2}$ and $Ti2p_{1/2}$ peaks changed from TiO to TiO_2 and from Ti_2O_3 to TiO_2, respectively. Examination of the plasma-treated titanium surface revealed that the oxide layer components had transformed into TiO_2. The results in the present study reveal that plasma oxidation transformed the substoichiometric titanium oxide into the stoichiometric titanium oxide (TiO_2). It reported the improved bonding of titanium to bone with TiO_2 layer [22]. Furthermore, implant alloy with plasma discharging and electro-discharging is believed to have excellent surface properties, thus enhancing biocompatibility and osseointegration [28,30]. As mentioned above, they indicate that some of the introduced oxygen atoms segregate as impurities at the interstitial sites and grain boundaries in the titanium surface. Plasma oxidation can efficiently form a dense oxidation film on implant surface. The effects of atomic mixing and/or ion bombardment and plasma-induced surface reactions were observed during plasma discharging. Hence, the effects induced by plasma discharging and plasma densification produce a smooth and functionalized surface.

Fig. 6(a) through (c) shows the SEM observations of cell morphology of Ti–6Al–4V after 48 h culture with and without plasma oxidation, respectively. The cells exhibited good adhesion in Ti, O–Ti-1, O–Ti-2. Additionally, the cell distribution on O–Ti-1 and O–Ti-2 was better than that on Ti. For every 200 nm increase in the thickness of the titanium oxide film achieved by anodic oxidation, the ratio of absorbed proteins albumin/fibrinogen increased 7 times [23]. Further, an increase in the thickness of the titanium oxide film from 10 nm to 250 nm by a thermal oxidation process was associated with 1.5-fold increase in clotting time. The blood compatibility of implants with oxide film clearly improved as titanium oxide layer thickness increased [24]. As stated above, oxide formation on the implant surface can enhance biocompatibility and

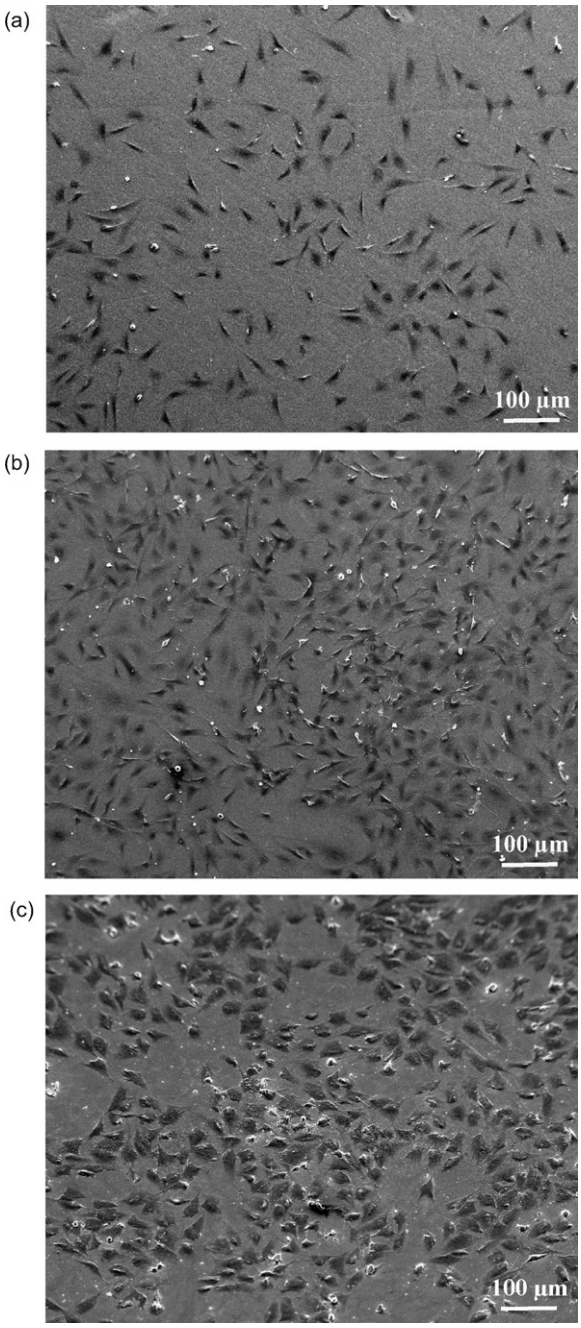

Fig. 6. SEM observations of cell morphology of (a) Ti, (b) O–Ti-1 and (c) O–Ti-2 after culturing for 48 h.

hemocompatibility. The numbers of cells associated with Ti and O–Ti-1 and O–Ti-2 were also investigated. After 8 h of culturing, the cells had attached and adhered but had not significantly spread. The number of attached bone-derived cells only slightly affected the dispersion of the attached cells. After 12 h of culture, the cells had spread to virtually all of the studied surfaces. More cells adhered to the O–Ti-1 and O–Ti-2 than to the Ti. The attachment assay with 24 h culture demonstrated that significantly ($p < 0.01$) more cells attached to the O–Ti-1 and O–Ti-2 than to the Ti. However, the O–Ti-1 has a homogenous cell distribution than that of O–Ti-2. Similar results were observed after culturing for 36 h and 48 h. The percentage of attached cells substantially exceeded the number attached to Ti. As indicated above, the cells spread over the oxida-

tion Ti surface more rapidly than on the machined titanium surface. Moreover, the cells on the treated surfaces reached confluence more quickly [6–10,12,28,30]. Based on the above investigation, the properties of oxidation layer may interpret the good biocompatibility of titanium implants. The oxide thickness obviously results in changes of the surface properties, whereas a phase transition will alter the cell reaction and distribution [8,10,28,30]. In the present study, formation of a nanostructural rutile-TiO_2 on oxidation layer is related with the cell and blood reaction and distribution selectivity, then promoting hemocompatibility and protein binding as well as osseointergration.

4. Conclusion

In the present study, oxygen plasma discharging was applied on titanium bone plates for forming a biocompatible layer. Plasma discharging formed a oxidation layer containing nanostructure and nanophase on the titanium. The nanostructural oxidation layer revealed oxygen and titanium bonding states following oxygen plasma discharging. A $(\alpha \rightarrow (\alpha + TiO) \rightarrow (\alpha + TiO + \gamma\text{-}TiO_2))$ phase transition was observed within the titanium matrix during plasma discharging. This result has never been previously reported. Plasma oxidation not only produces titanium oxide layer, but also results in formation of nanostructural γ-TiO_2. Nano-γ-TiO_2 phase can be enhanced osseointegration of implant such as orthopedic and dental implants. Surface oxidation by plasma discharging is thus believed to improve the biocompatibility and tissue healing. Furthermore, plasma discharging not only enhances phase transformation on titanium surface, but also generates a nanostructural oxide layer, improving the bioactivity and hemocompatibility of bone plate.

Acknowledgements

The authors would like to thank the National Science Council of Republic of China for financially supporting this research under contract No. NSC95-2622-B-038-005-CC3 and supporting by Hung Chun Bio-S Co. Ltd.

References

[1] P.I. Brånemark, J. Prosthet. Dent. 59 (1983) 399.
[2] P. Li, P. Ducheyne, J. Biomed. Mater. Res. 41 (1998) 341.
[3] H.C. Cheng, S.Y. Lee, C.M. Tsai, C.C. Chen, K.L. Ou, Electrochem. Solid-State Lett. 9 (2006) D25.
[4] H.C. Cheng, S.Y. Lee, C.C. Chen, Y.C. Shyng, K.L. Ou, Appl. Phys. Lett. 89 (2006) 173902.
[5] Y.H. Shih, C.T. Lin, C.M. Liu, C.C. Chen, C.S. Chen, K.L. Ou, Appl. Surf. Sci. 253 (2007) 3678.
[6] H.C. Cheng, S.Y. Lee, C.C. Chen, Y.C. Shyng, K.L. Ou, J. Electrochem. Soc. 154 (1) (2007) E13.
[7] K.L. Ou, G.T. Lin, S.L. Chen, C.F. Huang, H.C. Cheng, Y.M. Yeh, K.H. Lin, J. Electrochem. Soc. 155 (2008) E79.
[8] H.M. Kim, H. Kaneko, M. Kawashita, T. Kokubo, T. Nakamura, Key Eng. Mater. 254–256 (2004) 741.
[9] H.M. Kim, T. Himeno, M. Kawashita, J.H. Lee, T. Kokubo, T. Nakamura, J. Biomed. Mater. Res. 67A (2003) 1305.
[10] R. Mcpherson, N. Gane, T.J. Bastow, J. Mater. Sci.: Mater. Med. 15 (2004) 1237.
[11] H. Kurzweg, R.B. Heimann, T. Troczynski, J. Mater. Sci.: Mater. Med. 9 (1998) 9.
[12] H.M. Kim, F. Miyaji, T. Kuokubo, T. Nakamura, J. Biomed. Mater. Res. 32 (1996) 409.
[13] H.M. Kim, F. Miyaji, J. Mater. Sci.: Mater. Med. 8 (1997) 341.
[14] G.R. Vardiman, R.A. Kant, J. Appl. Phys. 53 (1982) 690.
[15] M.T. Pham, W. Matz, H. Reuther, E. Richter, G. Steiner, S. Oswald, J. Mater. Sci. Lett. 19 (2000) 443.
[16] K. Teii, S. Matsumoto, J. Robertson, Appl. Phys. Lett. 92 (2008) O13115.
[17] K. Teii, R. Yamao, T. Yamamura, S. Matsumoto, J. Appl. Phys. 101 (2007) 033301.
[18] K. Teii, M. Hori, M. Ito, T. Goto, N. Ishii, J. Vac. Sci. Technol. A 18 (2000) 1.
[19] K. Teii, T. Ikeda, Appl. Phys. Lett. 90 (2007) 111504.
[20] B.O. Aronsson, J. Lausmaa, B. Kasemo, J. Biomed. Mater. Res. 35 (1997) 49.
[21] C. Larsson, P. Thomsen, J. Lausmaa, M. Rodahl, B. Kasemo, L.E. Ericson, Biomaterials 15 (1994) 1062.
[22] K.A. Thomas, J.F. Kay, S.D. Cook, M. Jarcho, J. Biomed. Mater. Res. 21 (1987) 1395.
[23] B. Groessner-Schreiber, R.S. Tuan, J. Cell Sci. 101 (1992) 209.
[24] A.P. Serro, A.C. Fernandes, B. Saramago, J. Lima, M.A. Barbosa, Biomaterials 18 (14) (1997) 963.
[25] B. Yang, M. Uchida, H.M. Kim, X. Zhang, T. Kuokubo, T. Nakamura, Biomaterials 25 (2004) 1003.
[26] S.L. Chen, M.H. Lin, C.C. Chen, K.L. Ou, J. Alloy Compd. 456 (2008) 413.
[27] C.C. Chen, C.T. Lin, S.Y. Lee, L.H. Lin, C.F. Hunag, K.L. Ou, Appl. Surf. Sci. 253 (2007) 5173.
[28] C.C. Lin, H.C. Cheng, C.F. Huang, C.T. Lin, S.Y. Lee, C.S. Chen, K.L. Ou, J. Appl. Phys. 44 (12) (2005) 8590.
[29] T.J. Webster, E. Celaletdin, R.H. Doremus, R.W. Siegel, R. Bizios, Biomaterials 21 (2000) 1803.
[30] K.L. Ou, Y.H. Shih, C.F. Huang, C.C. Chen, C.M. Liu, Appl. Surf. Sci. 255 (2008) 2046.